



## Invited Paper

## Strict dual-mode large-mode-area fiber with multicore structure



Wenxing Jin <sup>a,b,\*</sup>, Guobin Ren <sup>a,b</sup>, Wei Jian <sup>a,b</sup>, Youchao Jiang <sup>a,b</sup>, Yue Wu <sup>a,b</sup>, Yuguang Yang <sup>a,b</sup>,  
Ya Shen <sup>a,b</sup>, Shuisheng Jian <sup>a,b</sup>

<sup>a</sup> Key Lab of All Optical Network & Advanced Telecommunication Network of EMC, Beijing Jiaotong University, Beijing 100044, China

<sup>b</sup> Institute of Lightwave Technology, Beijing Jiaotong University, Beijing 100044, China

## ARTICLE INFO

## Article history:

Received 29 September 2015

Received in revised form

10 January 2016

Accepted 11 January 2016

Available online 20 January 2016

## Keywords:

Multicore fiber

Dual-mode

Large mode area

Bending loss

## ABSTRACT

In this paper, we proposed a new kind of quasi-37-cores fiber structure consisting of 15 conventional cores and 22 air-hole cores. Strict dual-mode condition is systematically analyzed about three structure parameters, core-to-core pitch, relative core diameter, and difference of refractive index between core and cladding. Large effective area about  $1910.98 \mu\text{m}^2$  with low bending loss less than  $10^{-3} \text{ dB/m}$  is achieved while keeping strict dual-mode. This structured fiber has a great potential in high power fiber lasers and amplifiers.

© 2016 Elsevier B.V. All rights reserved.

## 1. Introduction

To overcome the capacity limit on current optical communication systems, multicore fiber (MCF) used in space division multiplexing (SDM) is seen as a potential candidate for increasing the capacity of telecommunication systems [1–5]. It is reported that 305 Tb/s SDM transmission results with 19 cores have been successfully achieved [6]. Meanwhile, large-mode area fiber has attracted researchers' attentions because of its advantage of reducing nonlinearity that imposes the primary limit on fiber capacity [7–9]. However, the differential modal group delay (DMGD) among the modes in conventional MCF is still a big challenge. So it is a necessary concern to get large effective mode area while keeping less modes. Recently, there have been significant interests in large mode area MCF [10–12]. Compared to conventional fiber structure, there are more design freedom degrees in MCF, such as core numbers, diameter of core, core-to-core pitch, refractive index difference between core and cladding and so on. In addition, the introduction of air-hole cores brings in an additional design degree. The flexible structure design with air-hole cores in MCF gives us a novel idea to suppress high-order modes [13] while pursuing large mode area. And quasi-19-cores fiber with air-hole cores structure supporting both strict dual-mode operation and

large effective mode area has been achieved by original design [14]. Therefore, it is a deserving study to optimize the structure of MCF so as to decrease the number of high-order modes and obtain large mode area.

In this paper, a novel quasi-37-cores fiber consisting of 15 conventional cores and 22 air-hole cores structure is proposed. Here, we focus on achieving large effective area with two strict dual-mode environment. We get optimized fiber based on three design freedom degrees: core-to-core pitch  $\Lambda$ , relative core diameter  $f$ , and difference of refractive index between core and cladding  $\Delta n$ . Detail analyses on mode properties and effective area of fundamental mode  $A_{\text{eff}}$  are discussed systematically. Large effective area about  $1910.98 \mu\text{m}^2$  can be achieved with strict dual-mode operation and low bending loss. This new kind of fiber can be useful for high power fiber lasers and amplifiers.

## 2. Fiber structure and design consideration

The proposed strict dual-mode large-mode-area fiber structure whose cores are arrayed in hexagon is shown in Fig. 1. Different from conventional MCF, the proposed fiber consists of 15 conventional cores in center and 22 air-hole cores that are equally arranged on both sides. These air-hole cores are able to make a leakage channels for high-order modes and those modes whose mode field distributions are likely to that of TE and TM modes. The blue small circle part represents conventional cores, the white small circle part represents air-hole cores, and the rest part represents the cladding of the fiber. The diameter of conventional cores and air-hole cores  $d$  is assumed to be equal. There are some

\* Corresponding author at: Institute of Lightwave Technology, Beijing Jiaotong University, Beijing 100044, China.

E-mail addresses: [13111011@bjtu.edu.cn](mailto:13111011@bjtu.edu.cn) (W. Jin), [gbren@bjtu.edu.cn](mailto:gbren@bjtu.edu.cn) (G. Ren), [wjian@bjtu.edu.cn](mailto:wjian@bjtu.edu.cn) (W. Jian), [13111018@bjtu.edu.cn](mailto:13111018@bjtu.edu.cn) (Y. Jiang), [14111015@bjtu.edu.cn](mailto:14111015@bjtu.edu.cn) (Y. Wu), [13111012@bjtu.edu.cn](mailto:13111012@bjtu.edu.cn) (Y. Yang), [13111014@bjtu.edu.cn](mailto:13111014@bjtu.edu.cn) (Y. Shen), [ssjian@bjtu.edu.cn](mailto:ssjian@bjtu.edu.cn) (S. Jian).

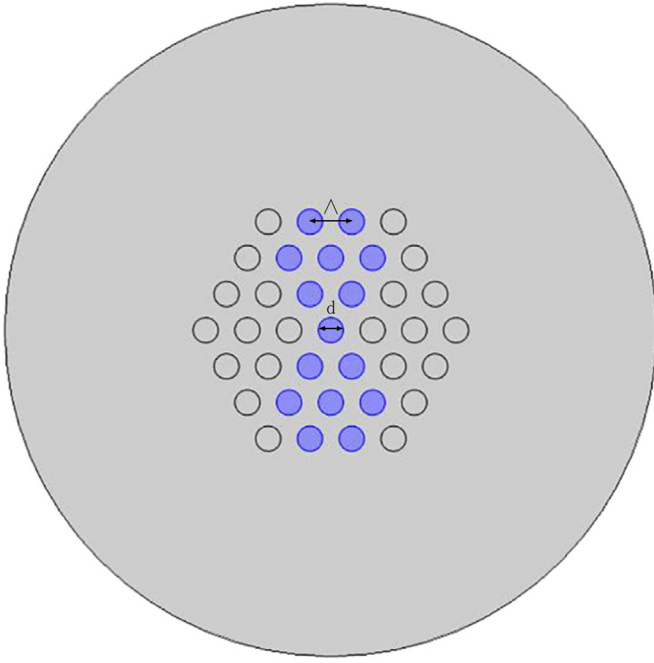


**Fig. 1.** Cross section schematic of proposed fiber structure. (For interpretation of the references to color in this figure caption, the reader is referred to the web version of this paper.)

parameters firstly presented: the cladding index of pure silica glass is  $n_{cl} = 1.444$ , the refractive index of air-hole cores is  $n_{air} = 1.000$ , and the refractive index of conventional cores is  $n_{co}$ . The index difference between core and cladding is defined as  $\Delta n = n_{co} - n_{cl}$ . In addition, core-to-core pitch  $\Lambda$  and relative core diameter  $f = d/\Lambda$  are also necessary structural variables.

To verify that the designed fiber can support two modes (including two degenerate modes  $HE_{11}$  and  $HE_{21}$ ) over C + L band, the effective indexes of modes are calculated for different wavelengths. For guided modes propagating along the fiber, the condition  $n_{cl} < n_{eff} < n_{co}$  must be satisfied. The modes with lower effective index than the cladding is to be cut off. The simulation results are obtained with the commercial software Comsol Multiphysics based on fully vectorial finite element calculations method. In addition, a user-defined and a circular perfectly matched layer (PML) is used. Fiber structural parameters are assumed as follows:  $\Lambda = 8.0 \mu\text{m}$ ,  $d = 4.8 \mu\text{m}$ ,  $f = 0.6$ ,  $\Delta n = 0.3\%$ . For each mode, we can get the effective refractive index from the following equation:

$$n_{eff} = \text{Re}\left(\frac{\beta}{k_0}\right) \quad (1)$$

where  $\beta$  is the propagation constant,  $k_0 = 2\pi/\lambda$ .

Fig. 2 shows the effective index  $N_{eff}$  of two modes in the fiber over various wavelengths  $\lambda$ . The calculating result indicates that only two degenerate modes ( $HE_{11}$  and  $HE_{21}$ ) can exit in the proposed fiber whose effective indexes are in the range of  $n_{cl}$  and  $n_{co}$ . The effective indexes of higher-order modes are lower than  $n_{cl}$ , so higher-order modes cannot exist in the fiber. At the same time, we get the birefringence  $HE_{11}$  mode is  $B_1 = |n_{eff-1-x} - n_{eff-1-y}| = |1.4445147 - 1.4445183| = 3.6 \times 10^{-6}$ , while the birefringence of  $HE_{21}$  mode is  $B_2 = |n_{eff-2-x} - n_{eff-2-y}| = |1.4444673 - 1.4444699| = 2.6 \times 10^{-7}$ . The birefringences of both two degenerate modes are less than  $10^{-5}$  that could be neglected compared to polarization-maintaining fiber whose birefringence always reaches  $10^{-4}$ . And that is why there is only one effective index line of each mode

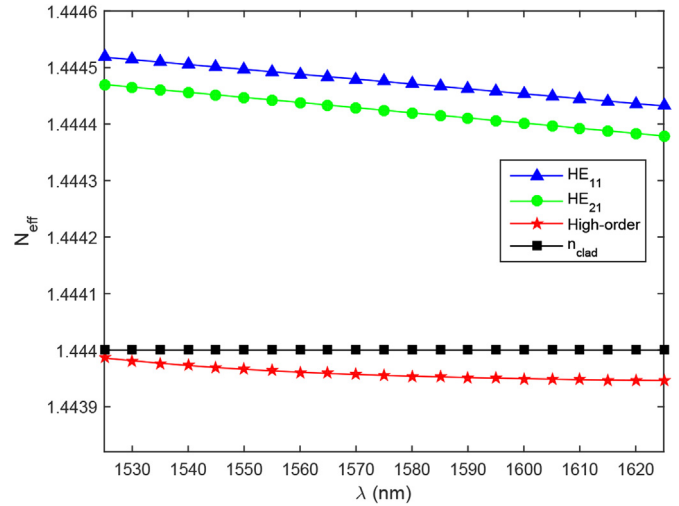


**Fig. 2.** Effective index  $N_{eff}$  of different modes at various operating wavelengths  $\lambda$ .

in Fig. 2. The high-order mode in Fig. 2 refers to the mode whose effective index is closest to  $HE_{21}$  mode. So strict dual-mode in this paper refers to the four vectorial modes: two degenerate  $HE_{11}$  modes and two degenerate  $HE_{21}$  modes.

The mode field distribution and 2-D electric vector distribution of each mode are displayed in Fig. 3. According to Fig. 3, it can be clearly seen that each mode has two degenerate modes of x-polarization mode and y-polarization mode. The mode field effective area of fundamental modes can be calculated as follows [10]:

$$A_{eff} = \frac{\int (E E^* dA)^2}{\int (E E^*)^2 dA} \quad (2)$$

where  $E$  represents the electric field and  $E^*$  represents the complex conjugate.

### 3. Structural parameters influence on mode area

Here we investigate three structural parameters: core-to-core pitch  $\Lambda$ , relative core diameter  $f$ , and difference of refractive index between core and cladding  $\Delta n$ . Here we also call  $HE_{11}$  mode fundamental mode. These three design freedom degrees can influence the number of modes and effective area of fundamental mode. The wavelength is fixed at 1550 nm unless otherwise specified.

At first, assuming that  $f = 0.6$ ,  $\Delta n = 0.3\%$ , the effective index of different modes  $N_{eff}$  various core-to-core pitch  $\Lambda$  is shown in Fig. 4 (a). Ignoring the birefringence of each mode that is less than  $10^{-5}$ , we can see that the effective index  $N_{eff}$  of each mode increases as core-to-core pitch  $\Lambda$  increases. As we know,  $f = d/\Lambda$ , the core diameter increases with the increment of  $\Lambda$  when relative core diameter  $f$  is fixed. We contribute the increase of  $N_{eff}$  to the increment of the equivalent core size with  $\Lambda$ . Meanwhile we notice that when  $\Lambda$  is less than  $0.6 \mu\text{m}$ , no mode exists. Two modes can be maintained as  $\Lambda$  is between  $6.2 \mu\text{m}$  and  $8.2 \mu\text{m}$ . And high-order modes show up when  $\Lambda$  is higher than  $8.2 \mu\text{m}$ . Fig. 4(b) shows the dependence of  $A_{eff}$  and  $N_{eff}$  on  $\Lambda$  in dual-mode condition. Here  $A_{eff}$  denotes the effective mode area of fundamental mode and  $\Delta N_{eff}$  represents the effective index difference between  $HE_{11}$  mode and  $HE_{21}$  mode. The diameter of each core increases with the increment of  $\Lambda$ , so  $A_{eff}$  increases with increment of each core size. That is to say,  $A_{eff}$  increases with the increment of  $\Lambda$ . From Fig. 4(b), one can see that  $A_{eff}$  gradually increases while  $\Delta N_{eff}$  slowly decreases with the increment of  $\Lambda$ . As a result,  $A_{eff}$  is able to achieve  $676.63 \mu\text{m}^2$  while  $\Lambda$  comes to  $8.2 \mu\text{m}$ , and  $\Delta N_{eff}$  has weak dependence on  $\Lambda$ .

Download English Version:

<https://daneshyari.com/en/article/1533425>

Download Persian Version:

<https://daneshyari.com/article/1533425>

[Daneshyari.com](https://daneshyari.com)